63234

A. R. A. P.

AERONAUTICAL RESEARCH ASSOCIATES *of* PRINCETON, INC.

AFOSR TN 60-1227 CONTRACT AF 49(638)-255

(ARAP Report No. 50)

EXAMINATION OF THE SOLUTIONS OF THE NAVIER-STOKES EQUATIONS FOR A CLASS OF THREE-DIMENSIONAL VORTICES

Part II: Velocity and Pressure Distributions for Unsteady Motion

by
Coleman duP. Donaldson
and
Roger D. Sullivan

Prepared for
Air Force Office of Scientific Research
Air Research and Development Command
United States Air Force
Washington 25, D. C.

November 1962

Aeronautical Research Associates of Princeton, Inc.
50 Washington Road, Princeton, New Jersey

ABSTRACT

The incompressible flow inside a porous cylindrical tube having steady radial inflow and rotating about its axis in a sinusoidal manner is obtained through solution of the complete Navier-Stokes equations. The nature of the tangential velocity profiles that result and the magnitudes of the mean pressure drop and the amplitude of the pressure fluctuations that are induced by the tangential velocities are discussed in some detail.

TABLE OF CONTENTS

1. Introduction

In reference 1 (hereafter referred to as Part I) we considered the behavior of a class of three-dimensional steady solutions of the Navier-Stokes equations. The flows considered were those such that, in a cylindrical coordinate system (r, ϕ, z), the radial, tangential, and axial velocity distributions were of the form

$$u = u(r)$$

$$v = v(r)$$

$$w = z\bar{w}(r)$$

while the pressure distribution was of the form

$$p = c_1 z^2 + p_1(r) + p_2(r)$$

In the above expression for the pressure one may identify the term $c_1 z^2$ with the pressure necessary to sustain the axial velocities, the term $p_1(r)$ with the pressures necessary to sustain the radial motion, and the term $p_2(r)$ with the pressures necessary to sustain the tangential velocities.

This special class of steady solutions of the Navier-Stokes equations is such that the equations for the radial and axial components of velocity are decoupled from the equations governing the tangential velocity distribution and the distribution of pressure. Because of this decoupling of the equations, one finds that for very little additional labor one can obtain the behavior of a simple class of unsteady solutions of the Navier-Stokes equations; namely, solutions of the form

$$u = u(r)$$

$$v = v(r, t)$$

$$w = z\bar{w}(r)$$

$$p = c_1 z^2 + p_1(r) + p_3(r, t)$$

We see from the above expression for the pressure that the pressures necessary to sustain the axial and radial velocities are identical to those of the steady flows, as might be expected, and only the pressure necessary to sustain the tangential velocities $p_3(r, t)$ becomes dependent on both position and time.

As in Part I of this report, these flows may be visualized as the flow inside a cylindrical porous tube which is subject to a rotation about its axis which is some arbitrary function of time.

In what follows, we will report in some detail the behavior of these solutions when the porous tube is subjected to a sinusoidal oscillation about its axis.

2. Basic Equations

The basic equations governing the fluid motions that we wish to discuss (see Part I, Section 2) are

$$\frac{1}{r}\frac{d}{dr}(ru) + \bar{w} = 0 \tag{2.1}$$

$$u\frac{du}{dr} - \frac{1}{r}v^2 = -\frac{1}{\rho}\frac{\partial p}{\partial r} + \nu\frac{d}{dr}\left[\frac{1}{r}\frac{d}{dr}(ru)\right] \tag{2.2}$$

$$\frac{\partial v}{\partial t} + \frac{u}{r}\frac{\partial(rv)}{\partial r} = \nu\frac{\partial}{\partial r}\left[\frac{1}{r}\frac{\partial}{\partial r}(rv)\right] \tag{2.3}$$

$$zu\frac{d\bar{w}}{dr} + z\bar{w}^2 = -\frac{1}{\rho}\frac{\partial p}{\partial z} + \nu z\frac{1}{r}\frac{d}{dr}\left(r\frac{d\bar{w}}{dr}\right) \tag{2.4}$$

We note that Equations (2.2) and (2.4) which govern the radial and axial velocities and the boundary conditions to be applied to these equations, namely $u(0) = 0$, $u(R) = U$, $\bar{w}'(0) = 0$, and $\bar{w}(R) = 0$, are identical to those discussed in detail in Part I. The radial and axial components of the flow are therefore identical to those of the steady flows of Part I.

We now introduce the non-dimensional variables

$$x = (r/R)^2 \tag{2.5}$$

$$\tau = St/R \tag{2.6}$$

$$f(x) = -2ru/RS \tag{2.7}$$

$$h(x, \tau) = rv/RV \tag{2.8}$$

where S and V are velocities and R a length that will be defined later. In terms of these new variables, Equation (2.3) becomes

$$xh_{xx} + nfh_x = nh_\tau \tag{2.9}$$

where the subscripts indicate differentiation with respect to the variables x and τ and the parameter $n = RS/4\nu$ is a Reynolds number.

Now let R be the internal radius of a porous cylinder oscillating in such a manner that

$$v(R, t) = V \cos \omega t \tag{2.10}$$

Applying this boundary condition to $h(x, \tau)$ gives us

$$h(1, \tau) = \cos \Omega\tau \tag{2.11}$$

where $\Omega = R\omega/S$. We also require that the tangential velocity vanish at $r = 0$, so that we have

$$h(0, \tau) = 0 \tag{2.12}$$

If we write

$$h = \text{R.P.}\left\{\Lambda(x)e^{-i\Omega t}\right\} = \lambda \cos \Omega t + \mu \sin \Omega t \tag{2.13}$$

where $\Lambda(x) = \lambda(x) + i\mu(x)$, then Equation (2.9) becomes

$$x\Lambda'' + nf\Lambda' = -in\Omega\Lambda \tag{2.14}$$

The boundary conditions (2.11) and (2.12) are

$$\Lambda(0) = 0 \qquad \Lambda(1) = 1 \tag{2.15}$$

Let $\phi(x) = \alpha(x) + i\beta(x)$ be a solution of Equation (2.14) when $\phi(0) = 0$ and $\phi'(0) = 1$. Then the solution we require is

$$\Lambda(x) = \frac{\phi(x)}{\phi(1)}$$

or writing $\phi(1) = \alpha_1 + i\beta_1$ we have

$$\lambda(x) = \frac{\alpha_1\alpha + \beta_1\beta}{\alpha_1^2 + \beta_1^2} \tag{2.16}$$

$$\mu(x) = \frac{\alpha_1\beta - \beta_1\alpha}{\alpha_1^2 + \beta_1^2} \tag{2.17}$$

where $\alpha(x)$ and $\beta(x)$ are solutions of

$$x\alpha'' + nf\alpha' = n\Omega\beta \tag{2.18}$$

subject to $\alpha(0) = 0$ and $\alpha'(0) = 1$ and

$$x\beta'' + nf\beta' = -n\Omega\alpha \tag{2.19}$$

subject to $\beta(0) = 0$ and $\beta'(0) = 0$.

In order to use the results presented in this report it is necessary to specify the characteristic velocity S. As is discussed in Part I (p. 38), the characteristic velocity S is the numerical value of the axial velocity at $r = 0$ and $z = R$. The exact value of S in relation to the radial inflow or outflow at $r = R$ is obtained from the steady solution for the radial and axial velocities. Figure 2.1 is a plot of the ratio of $n/|UR/\nu| = S/4|U|$ as a function of $|UR/\nu|$ for the simple families of one-celled flows obtained from the studies reported in Part I. As is indicated in this figure, one-celled flows under conditions of outward radial flow exist for only a limited range of radial Reynolds number (for a more extended discussion see Part I). For this reason, we shall limit the computations and discussion to the case of radial inflows.

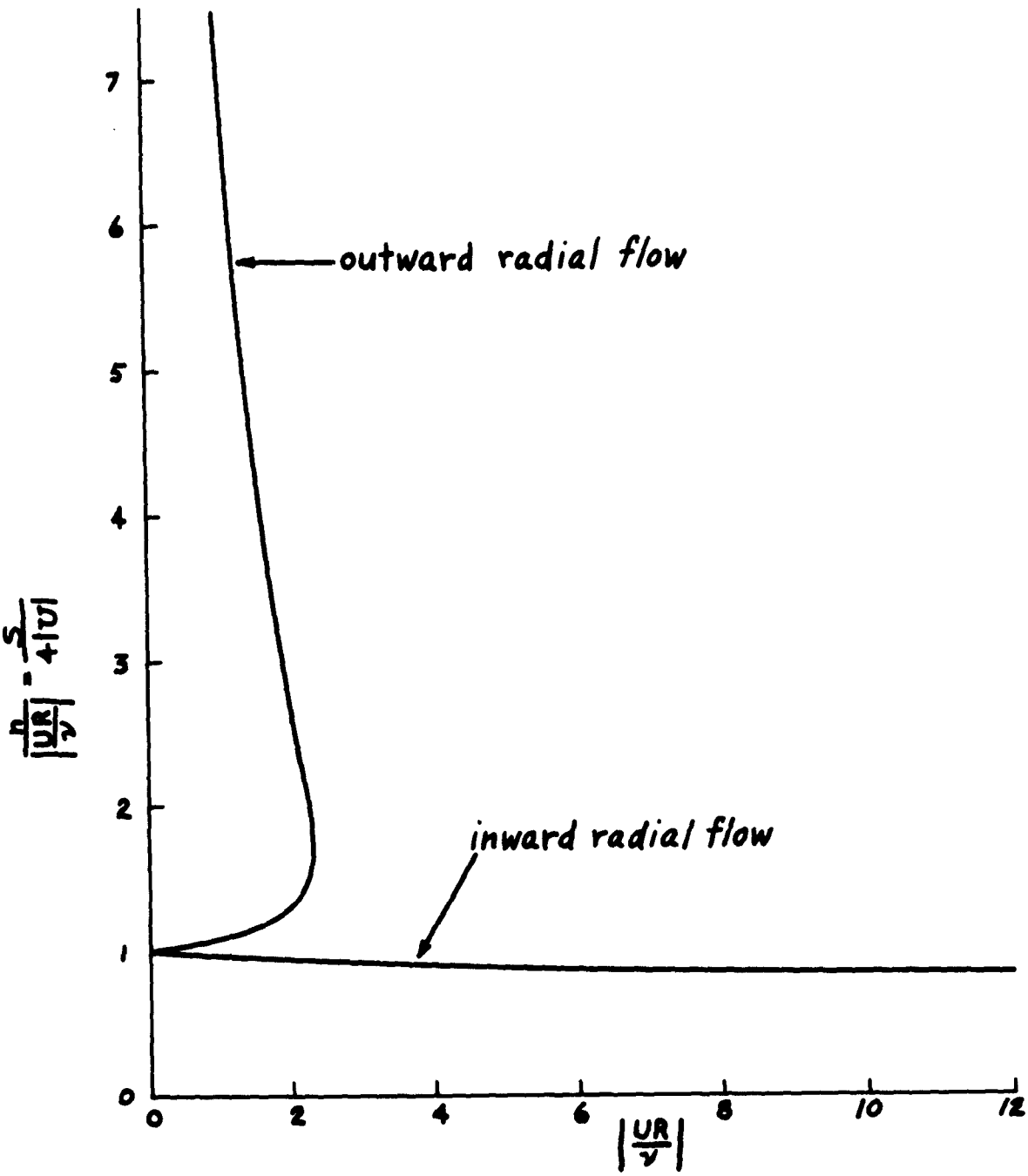

Fig. 2.1 Relationship between the characteristic velocity S and the numerical value of the radial velocity U into a porous cylinder of radius R as a function of the Reynolds number UR/ν .

3. Velocity Distributions

An analog computing machine was used to solve Equations (2.18) and (2.19) and thus determine the functions $\lambda(x)$ and $\mu(x)$ which represent the tangential velocity distribution, for a range of both the frequency parameter Ω and the Reynolds number n. In making these computations the radial velocity function $f(x)$ was generated by simultaneous solution of the appropriate equation for f subject to the proper boundary conditions (Equations (2.2.6), (2.2.8), (2.2.9), and (2.2.10) of Part I). Typical tangential velocity profiles at an instant in time and envelopes of the velocity profiles for all times are shown in Figures 3.1, 3.2, 3.3, and 3.4 with the Reynolds number n as a parameter for four values of the frequency parameter (Ω = 0, 0.3, 1.0, and 3.0 respectively). In Figure 3.5 the envelopes of the velocity profiles are shown for the particular Reynolds number $n = 10$ with Ω as a parameter.

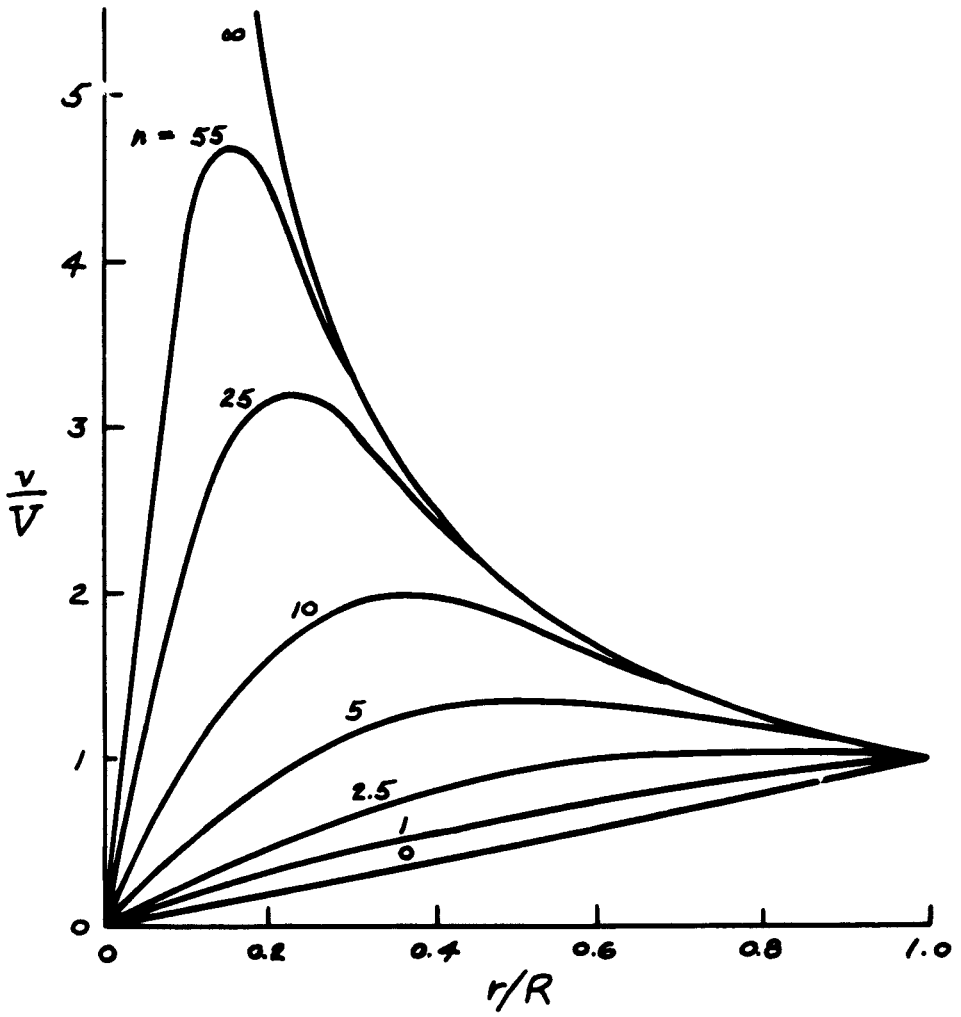

Fig. 3.1 Tangential velocity profiles $\Omega = 0$.

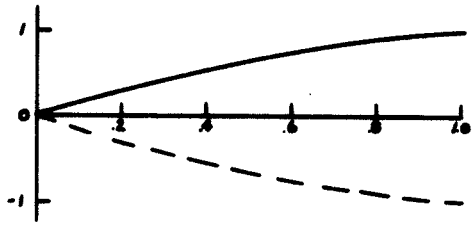

(a) n = 1

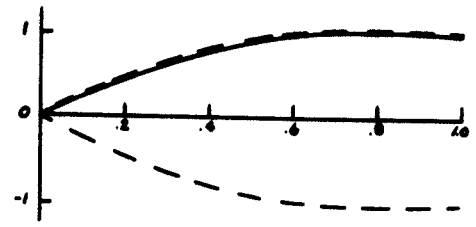

(b) n = 2.5

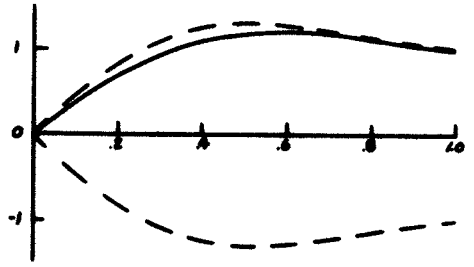

(c) n = 5

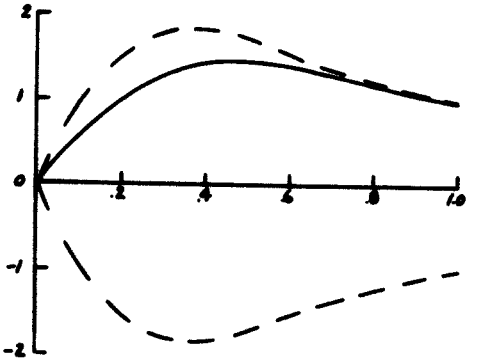

(d) n = 10

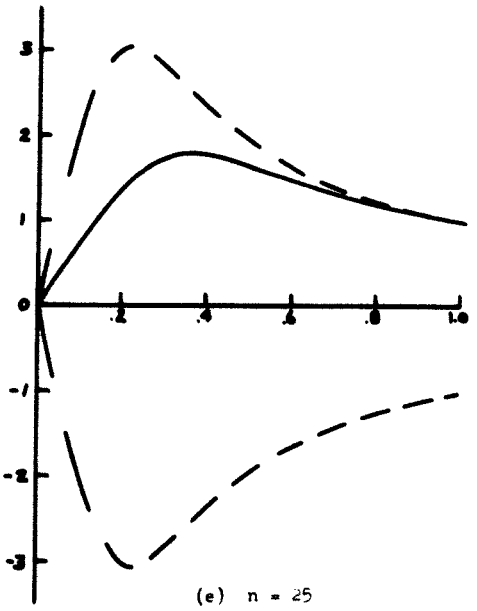

(e) n = 25

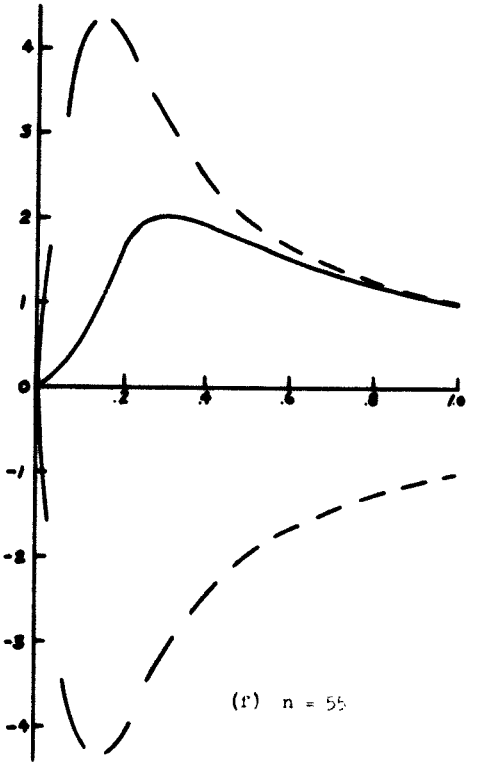

(f) n = 55

Fig. 3.2 Tangential velocity profiles Ω = 0.3.

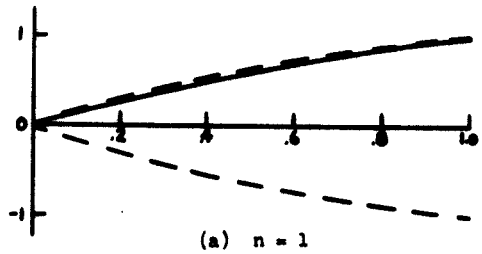

(a) n = 1

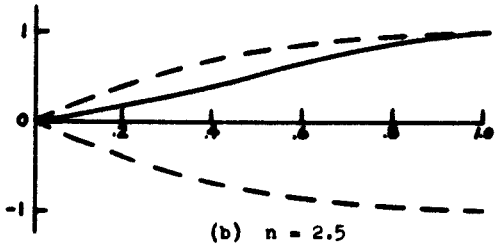

(b) n = 2.5

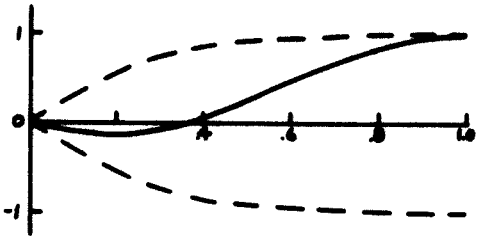

(c) n = 5

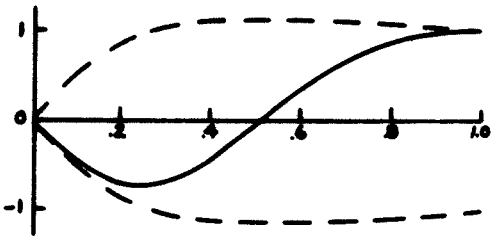

(d) n = 10

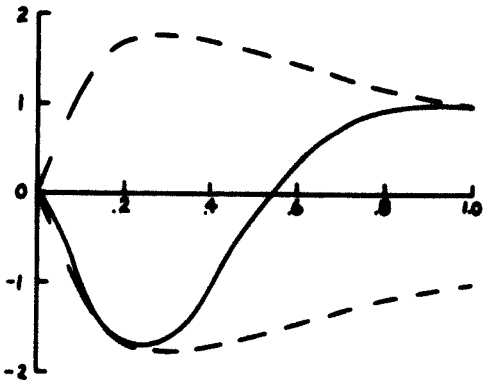

(e) n = 25

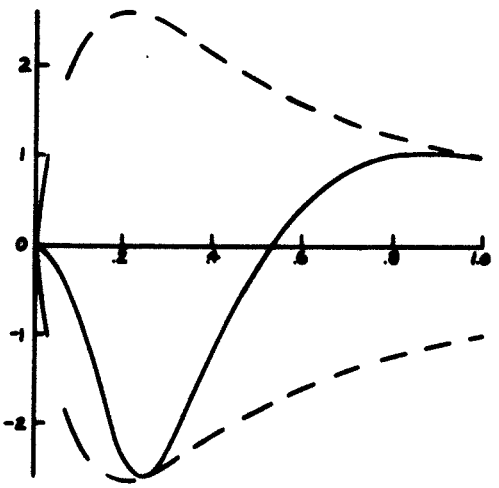

(f) n = 55

Fig. 3.3 Tangential velocity profiles $\Omega = 1.0$.

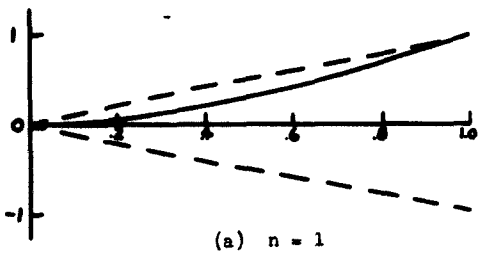

(a) n = 1

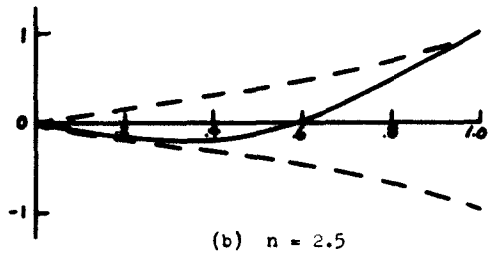

(b) n = 2.5

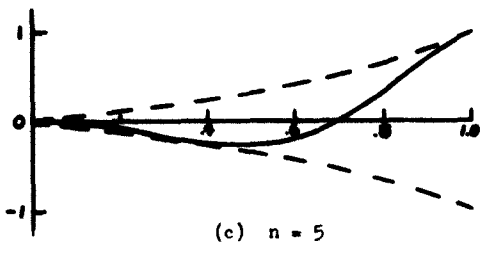

(c) n = 5

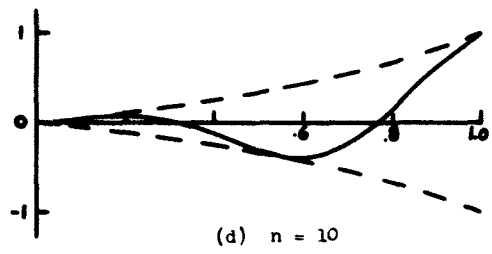

(d) n = 10

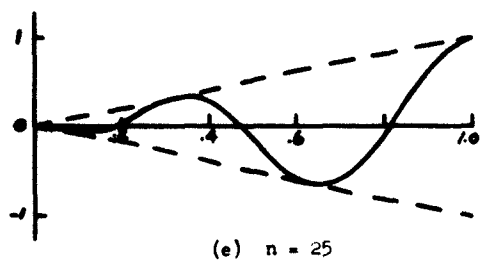

(e) n = 25

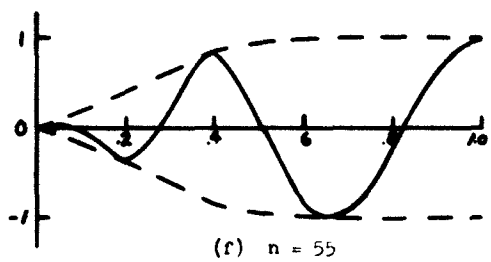

(f) n = 55

Fig. 3.4 Tangential velocity profiles Ω = 3.0.

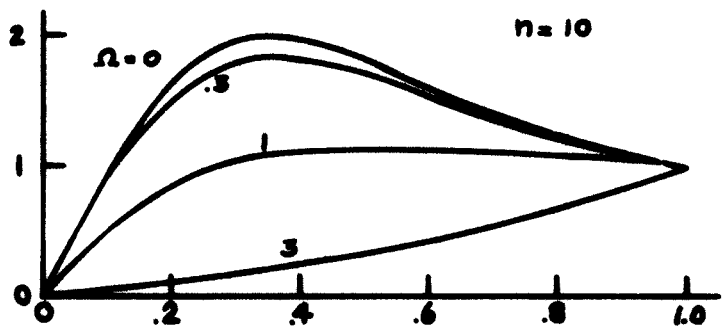

Fig. 3.5. Envelopes of the velocity profiles for $n = 10$ with Ω as a parameter.

4. Pressure Distributions

As pointed out in the introduction, the pressure distributions for the flows under discussion are of the form

$$p = c_1 z^2 + p_1(r) + p_3(r, t) \tag{4.1}$$

We may show this in the following manner. From Equation (2.2) we note, since u and v are functions of r alone, that $\partial^2 p/\partial r \partial z = 0$. Differentiating Equation (2.4) with respect to r gives

$$\frac{1}{\rho}\frac{\partial^2 p}{\partial r \partial z} = 0 = -z\frac{d}{dr}\left[u\frac{d\bar{w}}{dr} + \bar{w}^2 - \frac{\nu}{r}\frac{d}{dr}\left(r\frac{d\bar{w}}{dr}\right)\right] \tag{4.2}$$

From this equation we see that

$$u\frac{dw}{dr} + \bar{w}^2 - \frac{\nu}{r}\frac{d}{dr}\left(r\frac{d\bar{w}}{dr}\right) = \text{constant} \tag{4.3}$$

or

$$\frac{\partial p}{\partial z} = c_1 z \tag{4.4}$$

and

$$p = c_1 z^2 + \psi(r, t) \tag{4.5}$$

Since in what follows we are primarily interested in the effects of the tangential motions on the pressure we shall, in view of Equation (4.5), define

$$\pi(x, \tau) = \frac{p(x, z, \tau) - p(1, z, \tau)}{\rho} \tag{4.6}$$

In addition we define

$$\pi_{11}(x) = \int_1^x \frac{\lambda^2}{x^2}dx \tag{4.7}$$

$$\pi_{12}(x) = \int_1^x \frac{\lambda\mu}{x^2}dx \tag{4.8}$$

$$\pi_{22}(x) = \int_1^x \frac{\mu^2}{x^2}dx \tag{4.9}$$

$$\pi_3(x) = \frac{1}{8}\left[f^2(1) - \frac{1}{x}f^2(x)\right] \tag{4.10}$$

$$\pi_4(x) = -\frac{1}{4n}f'(x) \tag{4.11}$$

Substitution of Equations (4.6) through (4.11) into Equation (2.2) yields

$$\begin{aligned}\pi &= \tfrac{1}{2}V^2(\pi_{11}\cos^2\Omega\tau + 2\pi_{12}\sin\Omega\tau\cos\Omega t + \pi_{22}\sin^2\Omega\tau) + S^2(\pi_3+\pi_4)\\ &= \tfrac{1}{4}V^2\left[(\pi_{11}-\pi_{22})\cos 2\Omega\tau + 2\pi_{12}\sin 2\Omega\tau\right]\\ &\quad + \tfrac{1}{4}V^2(\pi_{11}+\pi_{22}) + S^2(\pi_3+\pi_4)\end{aligned} \tag{4.12}$$

In this equation, the term $S^2(\pi_3 + \pi_4)$ represents that part of the pressure required to sustain the radial motion, the term $S^2\pi_3$ representing the pressure due to inviscid effects and the term $S^2\pi_4$ representing the pressure due to viscous effects. The remaining terms on the right-hand side of Equation (4.12) represent the pressure required to sustain the tangential velocities. There are two effects:

a mean pressure difference

$$\frac{\Delta p_m}{\frac{1}{2}\rho V^2} = \frac{1}{2}(\pi_{11} + \pi_{22}) \tag{4.13}$$

and a fluctuation in pressure at twice the frequency of the oscillation of the porous boundary which has an amplitude

$$\frac{\left|\Delta p_f\right|_{max}}{\frac{1}{2}\rho V^2} = \frac{1}{2}\sqrt{(\pi_{11} - \pi_{22})^2 + 4\pi_{12}^2} \tag{4.14}$$

Figures 4.1 and 4.2 are plots of these two quantities evaluated at $r = x = 0$ as obtained from the analog solutions for λ and μ discussed in Section 3 for the Reynolds number range $0 < n \leq 55$ and for values of the frequency parameter equal to 0, 0.3, 1.0, and 3.0. For purposes of comparison, there is also plotted in Figures 4.1 and 4.2, the mean pressure drop and amplitude of the pressure fluctuation (which in the limiting case $\Omega \to 0$ is equal to the mean pressure drop) obtained from a form of Burgers' analytical solution (Reference 2) for the steady ($\Omega = 0$) tangential motion which is valid for large n, namely

$$\frac{v}{V} = \frac{1}{\sqrt{x}} \frac{1 - e^{-nx}}{1 - e^{-n}} \tag{4.15}$$

If Equation (4.15) is used to obtain Δp_m and $\left|\Delta p_f\right|_{max}$ for $\Omega \to 0$, there results

$$\frac{\Delta p_m}{\frac{1}{2}\rho V^2} = \frac{\left|\Delta p_f\right|_{max}}{\frac{1}{2}\rho V^2} = \frac{n}{2}\delta n\, 4 - \frac{1}{2} \qquad (n \gg 1)$$

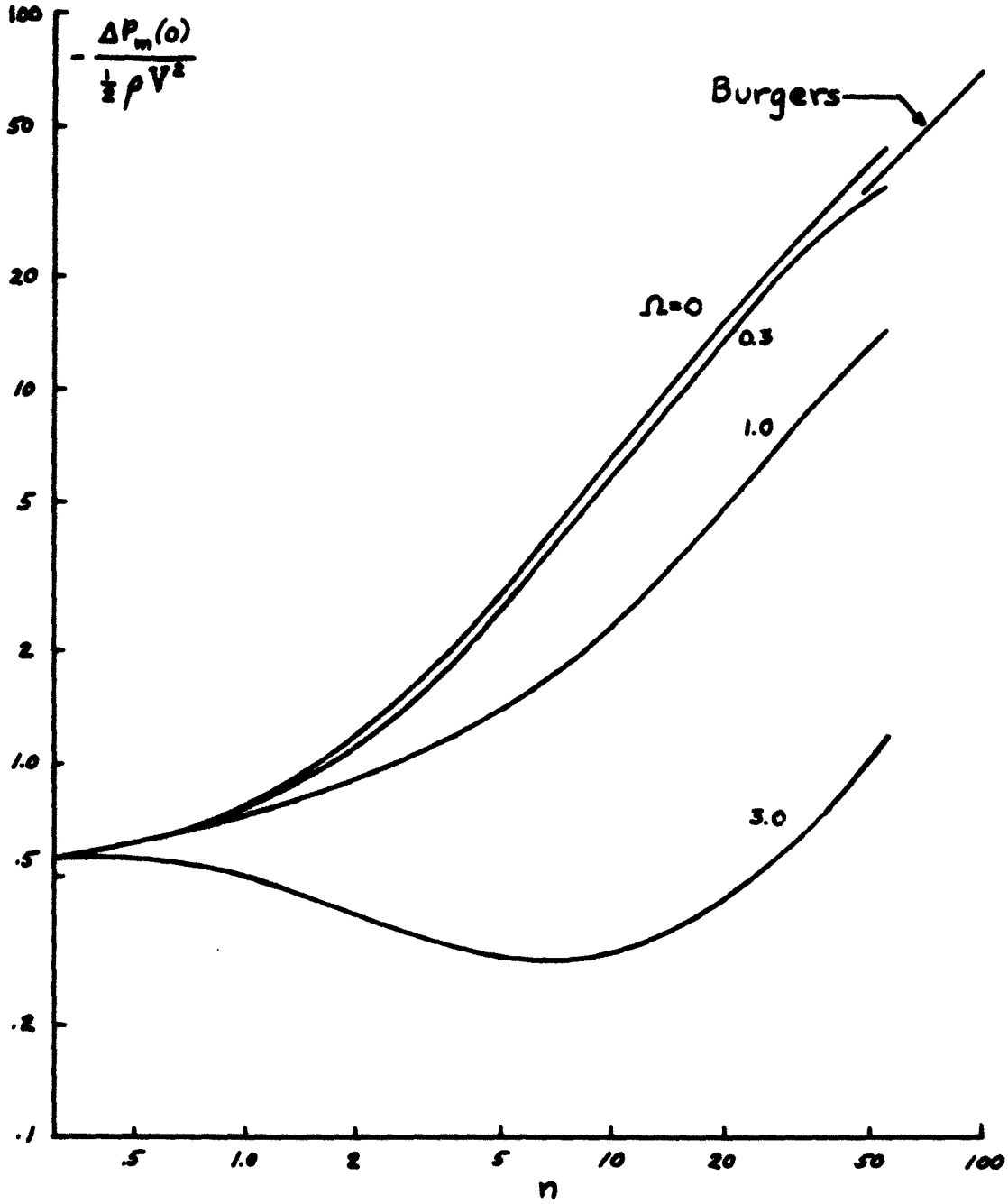

Fig. 4.1 Mean pressure drop in an oscillating vortex tube as a function of Reynolds number for various non-dimensional oscillatory frequencies Ω of the vortex tube.

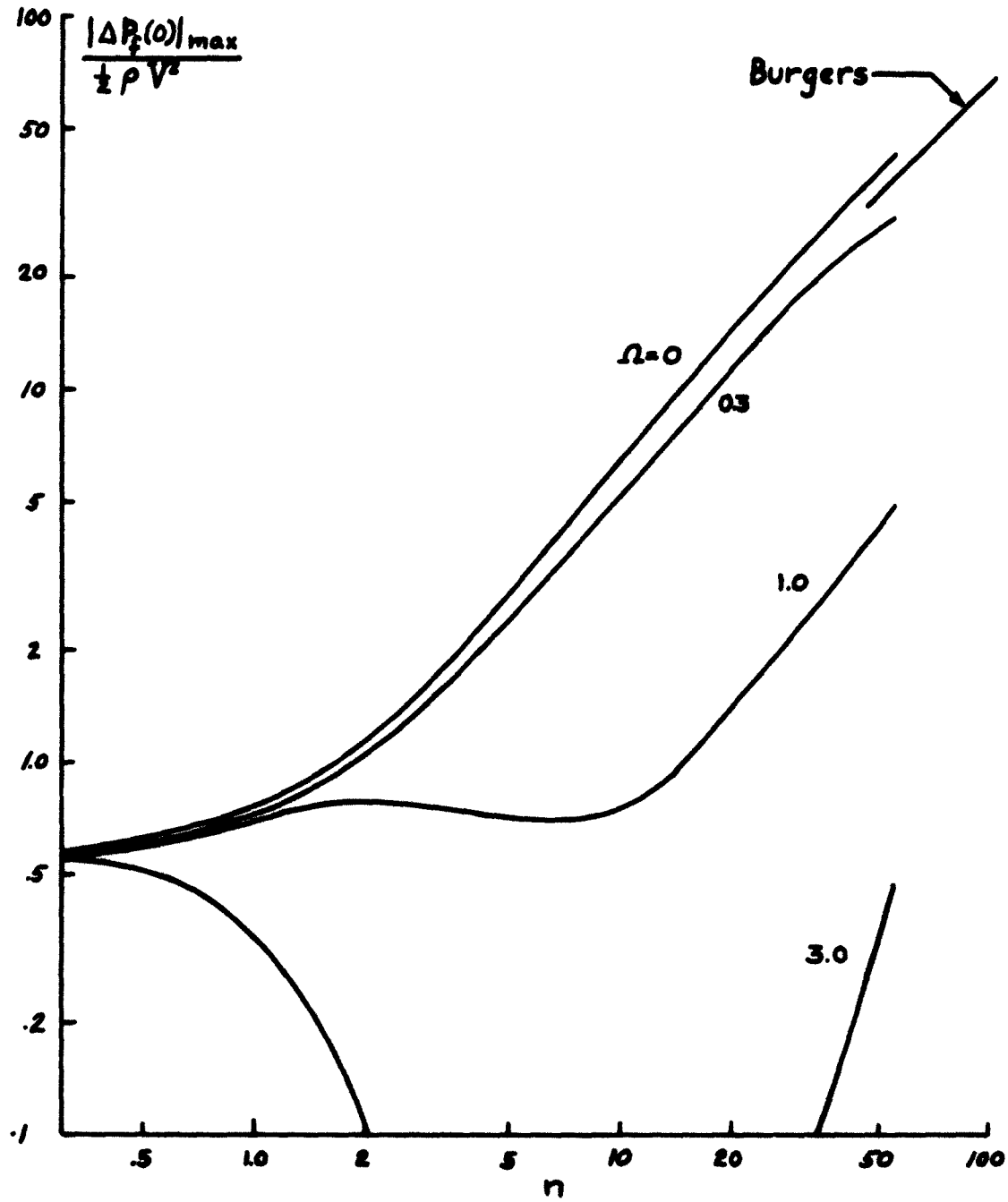

Fig. 4.2 Amplitude of the pressure fluctuation in an oscillating vortex tube as a function of Reynolds number for various non-dimensional frequencies Ω of the vortex tube. The non-dimensional frequency of the pressure fluctuation is 2Ω.

5. Discussion of Results

It is convenient to start the discussion of the results just presented with an analysis of Figures 4.1 and 4.2. We note that for $n \to 0$, $\Delta p_m(0)/\frac{1}{2}\rho V^2 = -0.5$ and $|\Delta p_f(0)|_{max}/\frac{1}{2}\rho V^2 = 0.5$. This is easily shown to be true because, in the limit of zero Reynolds number or infinite viscosity, the fluid within the vortex tube turns as a solid. Thus as $n \to 0$

$$v = v(R)\frac{r}{R} \tag{5.1}$$

and, from Equation (2.2), that portion of p that is due to the tangential velocity is then obtained from an integration of

$$\frac{dp}{dr} = \frac{\rho v^2}{r} \tag{5.2}$$

Substituting Equation (5.1) into (5.2) and integrating yields

$$p(0) - p(R) = -\tfrac{1}{2}\rho\left[v(R)\right]^2 \tag{5.3}$$

Since we have chosen $v(R) = V \cos \omega t$ we have

$$p(0) - p(R) = -\tfrac{1}{2}\rho V^2 \cos^2 \omega t \tag{5.4}$$

or

$$\frac{p(0) - p(R)}{\frac{1}{2}\rho V^2} = -\tfrac{1}{2}(1 + \cos 2\omega t)$$

Thus for $n \to 0$ the mean part of the non-dimensional pressure difference is -0.5 and the amplitude of the non-dimensional pressure fluctuation is 0.5. The frequency of the pressure fluctuation is twice the frequency of oscillation of the boundary.

Whether or not the mean pressure drop and the amplitude of the pressure fluctuations become larger numerically as the Reynolds number n is increased depends on the frequency

parameter Ω. For frequency parameters smaller than unity, the general trend is for the pressure difference and amplitude to increase numerically as n increases. As Ω becomes larger than unity, the tendency is for the mean pressure differences and amplitudes to at first decrease numerically as n becomes larger than unity and then finally increase at some Reynolds number. The Reynolds number at which the pressure fluctuations start to increase is a function of Ω. The larger Ω becomes, the larger is the range of n above unity for which the mean pressure differences and the amplitudes of the pressure fluctuations due to the oscillating boundary are of small magnitude. Eventually, for an incompressible fluid, all curves such as those shown in Figures 4.1 and 4.2 must turn upwards because, given any finite frequency no matter how high, one can always choose a Reynolds number high enough so that the shears developed between successive maxima of the velocity distribution curves become negligible. When this condition exists, the fluid introduced through the porous boundary is able to maintain to some degree its initial angular momentum with the result that high tangential velocities are carried toward the axis. In an incompressible medium these high tangential velocities cause pressure fluctuations that are transmitted instantaneously to the boundaries of the flow. It appears from what has been said above and from the behavior of the solutions which have been obtained, that for all finite frequencies the mean pressure difference and the amplitude of the pressure fluctuations become proportional to n as $n \to \infty$, as has been discussed for the case $\Omega = 0$ in Section 4.

The reason for the initial drop in the numerical values of $\Delta p_m(0)$ and $|\Delta p_f(0)|_{max}$ as n increases for frequency parameters greater the unity can best be explained as follows. At low Reynolds numbers ($n \ll 1$), the viscosity

of the fluid is so high that reasonably large tangential velocities are maintained all the way to the center of the vortex tube by strong viscous action. As the viscosity is decreased the fluid toward the center of the tube no longer feels so strongly the effect of the surrounding cylinder at $r = R$. However, the viscosity is such that the entering fluid can not retain its initial angular velocity. The result is that the velocities near the center of the tube are not as large as they are for $n = 0$ as may be seen from the tangential velocity envelope for $\Omega = 3.0$ and $n = 10$ shown in Figure 3.5. It should be obvious, for a fixed Reynolds number n, that the velocity profiles and their envelopes should become somewhat similar to those in the vicinity of an oscillating flat plate (see Reference 3) as Ω is increased to larger and larger values.

The reason for the slight discrepancy between the behavior of the mean pressure drop and the amplitude of the pressure fluctuations obtained from the analog computations and the analytical results obtained from Burgers' solution for $\Omega = 0$ was a first thought to be computational inaccuracy. After this possibility had been checked and the computational inaccuracies found to be far less than the amount of the discrepancy, it was realized that the discrepancy is due to the different radial velocity profiles for the two cases. In the case of Burger's solution, the radial velocity is of the form $u/u(R) = \sqrt{x}$, while for the cases investigated in this report, the appropriate limiting form of the radial velocity distribution as $n \to \infty$ is

$$\frac{u}{u(R)} = \frac{1}{\sqrt{x}} \sin\left(\frac{\pi x}{2}\right)$$

(see Part I, page 64). It is this difference in radial velocity distributions that is responsible for the differences in the two curves for $\Omega = 0$ and $n \to \infty$ in Figures 4.1

and 4.2.

It is interesting to note that for the particular case of flows for which the radial velocity at $r = R$ is proportional to the tangential velocity at $r = R$, the pressure fluctuations in the flow will vary as V^3 for high enough Reynolds number since, in this case, the Reynolds number n is proportional to V and, for high enough Reynolds number for a fixed frequency, $|\Delta p_f(0)|_{max}/\frac{1}{2}\rho V^2$ becomes proportional to n.

REFERENCES

1. Donaldson, Coleman duP. and Sullivan, Roger D. Examination of the Solutions of the Navier-Stokes Equations for a Class of Three-Dimensional Vortices, Part I: Velocity Distributions for Steady Motion. AFOSR TN 60-1227, October 1960.

2. Burgers, J. M. A Mathematical Model Illustrating the Theory of Turbulence. Adv. in Appl. Mech., Vol. I, pp. 197-199. Academic Press, 1948.

3. Schlichting, H. Boundary Layer Theory. McGraw-Hill, pp. 75-76, (1960).